Eur Biophys J (1998) 27: 514–520 © Springer-Verlag 1998

ARTICLE

David Odde

Diffusion inside microtubules

Received: 2 March 1998 / Revised version: 3 May 1998 / Accepted: 3 May 1998

Abstract Recent high-resolution analysis of tubulin's structure has led to the prediction that the taxol binding site and a tubulin acetylation site are on the interior of microtubules, suggesting that diffusion inside microtubules is potentially a biologically and clinically important process. To assess the rates of transport inside microtubules, predictions of diffusion time scales and concentration profiles were made using a model for diffusion with parameters estimated from experiments reported in the literature. Three specific cases were considered: 1) diffusion of $\alpha\beta$-tubulin dimer, 2) diffusion/binding of taxol, and 3) diffusion/binding of an antibody specific for an epitope on the microtubule's interior surface. In the first case tubulin is predicted to require only ~1 min to reach half the equilibrium concentration in the center of a 40 μm microtubule open at both ends. This relatively rapid transport occurs because of a lack of appreciable affinity between tubulin and the microtubule inner surface and occurs in spite of a three-fold reduction in diffusivity due to hindrance. By contrast the transport of taxol is much slower, requiring days (at nM concentrations) to reach half the equilibrium concentration in the center of a 40 μm microtubule having both ends open. This slow transport is the result of fast, reversible taxol binding to the microtubule's interior surface and the large capacity for taxol (~12 mM based on interior volume of the microtubule). An antibody directed toward an epitope in the microtubule's interior is predicted to require years to approach equilibrium. These results are difficult to reconcile with previous experimental results where substantial taxol and antibody binding is achieved in minutes, suggesting that these binding sites are on the microtubule exterior. The slow transport rates also suggest that microtubules might be able to serve as vehicles for controlled-release of drugs.

Key words Taxol · Tubulin · Antibody · Adsorption

D. Odde
Department of Chemical Engineering,
Michigan Technological University,
Houghton, MI 49931, USA

Introduction

Recent analysis of the role of translational diffusion in microtubule dynamics has focussed on the transport of tubulin from the surrounding fluid to the growing microtubule's tip (Dogterom et al. 1995; Odde 1997). The conclusion from these theoretical analyses was that microtubule assembly does not occur at diffusion-limited rates, but is possibly influenced by diffusion particularly when many microtubule tips are close together such as occurs near the centrosome or in kinetochores. To date no analysis of molecular diffusion inside microtubules has been reported, perhaps because there has not been any evidence that it has biological relevance. However, the recent determination of tubulin structure at 3.7-angstrom resolution led to the prediction that key sites on tubulin are in the interior of microtubules, including the sites for taxol and epothilone binding and tubulin acetylation (Nogales et al. 1998). This suggests that biologically-relevant sites are located in the interior of microtubules and raises the question of whether this prediction is consistent with predicted rates of intramicrotubule transport. Given that the 13 protofilament microtubule inner diameter is only ~17 nm (Amos 1979) while typical microtubule lengths are on the order of 1–100 μm, it seems that translational diffusion inside microtubules could potentially limit the rate at which molecules interact with interior sites.

To assess the role of diffusion inside microtubules, a mathematical model was developed that accounted for translational diffusion, wall-mediated hindrance, and fast, reversible binding to the microtubule walls at dilute concentrations. Rates of transport were predicted using experimentally-based parameter sets for three specific cases: tubulin, taxol, and an antibody specific for an interior epitope. From the analysis of taxol transport and comparison to available kinetic and thermodynamic data (Caplow et al. 1994; Salmon and Wolniak 1984), it seems unlikely that the taxol binding site is on the interior of microtubules. In addition, comparison to previous experiments with anti-acetylated tubulin antibodies (Schulze et al. 1987), it also

seems unlikely that the Lys40 residue on α-tubulin is located on the interior of microtubules. More generally, the analysis leads to the prediction that fast, reversible binding can reduce the transport rate by 6 orders of magnitude, so that hindrance, while reducing effective diffusivities by a factor of ~3 for large molecules like tubulin and antibodies, is a second-order effect compared to binding.

Model

Model with diffusion only

For one-dimensional, unsteady-state diffusion, a species mass balance leads to a governing differential equation, also known as Fick's second law,

$$\frac{\partial c}{\partial t} = D\,\frac{\partial^2 c}{\partial x^2} \tag{1}$$

where $c(x, t)$ is the concentration of diffusing solute at position x and time t, and D is the translational diffusivity of the solute in the solvent. For a microtubule of length l initially devoid of solute and then subjected to a step change in solute concentration in the surrounding bath, c_0, the initial condition is

$$\textit{I.C.} \qquad t = 0,\ c = 0 \qquad (\text{for } 0 \le x \le l) \tag{2}$$

and the boundary conditions, assuming one end (at $x = 1$) is open and the other closed (at $x = 0$; as might occur when embedded into a centrosome), are given by

$$\textit{B.C. 1} \qquad x = 0,\quad \frac{\partial c}{\partial x} = 0 \qquad (\text{for } t > 0) \tag{3}$$

$$\textit{B.C.2} \qquad x = l,\quad c = c_0 \qquad (\text{for } t > 0) \tag{4}$$

Then the concentration, $c(x, t)$, is given by (Crank 1975)

$$\frac{c}{c_0} = 1 - \frac{4}{p}\sum_{n=0}^{\infty}\frac{(-1)^n}{2n+1}\exp\{-D(2n+1)^2 p^2 t/4l^2\} \cdot \cos\frac{(2n+1)\,p\,x}{2l} \tag{5}$$

which is plotted in Fig. 1 as a function of dimensionless position, x/l, for increasing values of dimensionless time, Dt/l^2. The solution given by Eq. (5) and plotted in Fig. 1 can also be applied to a microtubule with both ends open. In this case the solution is applied to a microtubule of length $2\,l$ where the minimum concentration is at $x = 0$ and the maximum at $x = \pm 1$ where the concentration is c_0.

Model with hindered diffusion

Because the dimensions of the microtubule lumen are of macromolecular dimensions, there is additional friction exerted by the microtubule inner walls in opposition to Brownian motion, a phenomenon known as hindrance. Hindrance reduces the effective diffusivity for solutes of a size approaching that of the pore in which they are diffusing. To model hindrance in microtubules, the diffusing molecule was approximated as a sphere in a cylindrical pore. In this case the dependence of diffusivity on molecule size is fairly well-established and can be directly applied to diffusion inside microtubules. The well-established result of Renkin gives the diffusivity at the centerline of the cylinder (Renkin 1954)

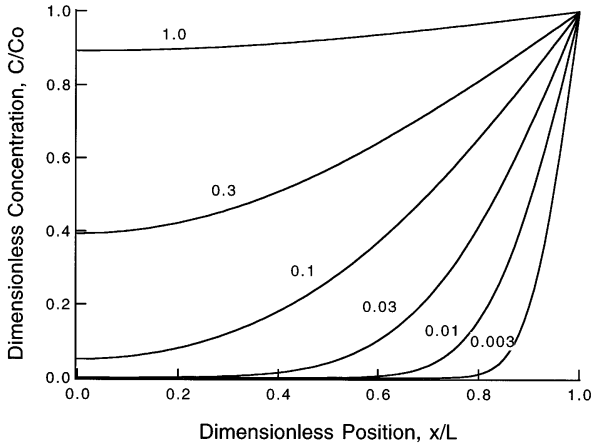

Fig. 1 Concentration profiles of molecules diffusing inside microtubules. The microtubule is assumed to be closed at $x = 0$ and open at $x = l$. Alternatively, for a microtubule open at both ends the model predictions can be used as well. In this case the concentration at $x = 0$ corresponds to the concentration in the middle of a microtubule having length $2\,l$. The curves represent the profile at various dimensionless times, Dt/l^2

$$\frac{D}{D_0} = 1 - 2.104\,\lambda + 2.09\,\lambda^3 - 0.95\,\lambda^5 \tag{6}$$

where λ is the molecular radius divided by the cylinder radius, D is the diffusivity in the cylinder, D_0 the diffusivity in the bulk fluid outside the cylinder.

Two problems with this frequently cited relation are: 1) it fails in the limit of $\lambda \to 1$ (Deen 1987), and 2) it overestimates the diffusivity in the limit of small λ (Nitsche and Balgi 1994). To overcome the first limitation the relation developed by Bungay and Brenner can be used instead (Bungay and Brenner 1973)

$$\frac{D}{D_0} = 6\pi\left(\begin{array}{l}\frac{9}{4}\pi^2\sqrt{2}(1-\lambda)^{-5/2}\left[1-\frac{73}{60}(1-\lambda)+\frac{77,293}{50,400}(1-\lambda)^2\right]-\ldots \\ \ldots-22.5083-5.6117\lambda-0.3363\lambda^2-1.216\lambda+1.647\lambda^4\end{array}\right)^{-1} \tag{7}$$

To overcome the second limitation, an asymptotic relation for small λ is given by Nitsche and Balgi (1994)

$$\frac{D}{D_0} = \left(1 + \frac{9}{8}\lambda\ln\lambda - 1.539\,\lambda + 1.2\,\lambda^2\right)\Big/(1-\lambda)^2 \tag{8}$$

The three relations given in Eqs. (6)–(8) are plotted in Fig. 2 over the full range of λ from 0 to 1. To model diffusion in microtubules, the Nitsche-Balgi relation was used for $\lambda < 0.2$ (i.e. for taxol) and the Bungay-Brenner relation used for $\lambda \ge 0.2$ (i.e. for tubulin and antibody). Based on

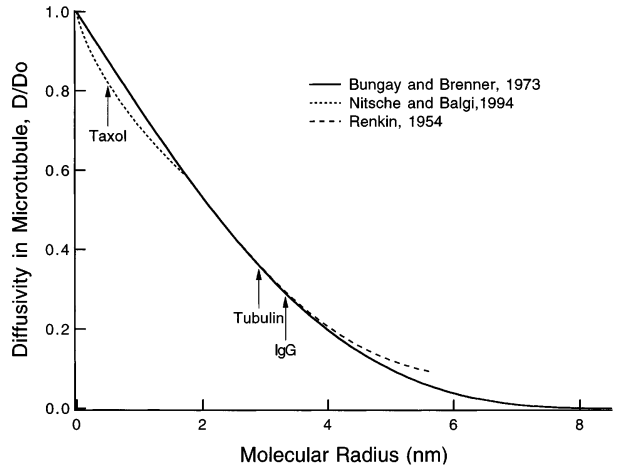

Fig. 2 Effect of hindrance on diffusivity as a function of molecular size. For larger molecules such as tubulin and IgG the effect of hindrance results in ~3-fold decrease in the diffusivity from that outside microtubules

electron crystallographic data, the radius of taxol was estimated to be 0.5 nm (Nogales et al. 1998). Tubulin was modelled as an ellipsoid with long dimension of 8 nm and short dimension of 4 nm, yielding an effective hydrodynamic radius of 2.9 nm (Berg 1993). Antibody size was estimated by scaling the tubulin radius using the ratio of the antibody molecular weight to the tubulin molecular weight (scaling = $(1.5)^{1/3} = 1.14$) to yield a molecular radius of 3.3 nm. Additional reductions in diffusivity occur in the cell due to higher intrinsic viscosity in the cytoplasm ($D/D_0 = 0.78$) and macromolecular occlusion ($D/D_0 = 0.40$) (Kao et al. 1993). Together these two effects accounted for a 3.2-fold decrease in the diffusivity from the value estimated for diffusion in water.

Model with diffusion and fast, reversible binding under dilute conditions

As molecules diffuse into the microtubule they can transiently adhere to the inner surface, thereby retarding their progress into the microtubule. This binding process can be idealized kinetically by the reversible reaction

$$A + B \underset{k_{off}}{\overset{k_{on}}{\rightleftharpoons}} AB \tag{9}$$

where A represents the diffusing solute, B a site on the interior of a microtubule, and AB a complex between the two. The forward and reverse rate constants, k_{on} and k_{off}, respectively, can be used to define an association equilibrium constant

$$K = \frac{k_{on}}{k_{off}} = \frac{[AB]}{[A][B]} = \frac{1}{K_D} \tag{10}$$

where K has units of M^{-1} and the dissociation equilibrium constant, K_D, has units of M (note that $c = [A]$). This type of binding gives rise to the Langmuir isotherm which relates the bound concentration of species A to the free concentration of species A at equilibrium by

$$q = \frac{n K [A]}{1 + K [A]} \tag{11}$$

where q is the bound concentration at equilibrium (M) and n the maximum bound concentration (M). To solve for the concentration profile of A in the case where binding can occur requires simultaneous solution of coupled nonlinear species mass balances on A and B with reaction terms included from Eq. (9). To keep the present analysis relatively simple, an asymptotic case was investigated where a closed-form analytical solution is obtainable, which is the case when A is dilute so that $[A] \ll K_D$. In this case the diffusivity is simply rescaled by a dimensionless equilibrium constant so that the D in Eq. (5) is replaced by an effective diffusivity (Crank 1975)

$$D_{eff} = \frac{D}{1 + K^*} \tag{12}$$

where K^* is given by

$$K^* = n K = \frac{n k_{on}}{k_{off}} \tag{13}$$

which relates the bound and free concentrations of A when $[A] \ll K_D$ (see Eq. (11). A key assumption in this modification to Eq. (5) is that the binding is not only reversible, but also faster than the diffusion transport rates.

Results

Model parameter estimates

A summary of parameter estimates is given in Table 1. The diffusivity of taxol was estimated using the Stokes-Einstein relation

$$D = \frac{k_B T}{6 \pi \mu R} \tag{14}$$

where k_B is the Boltzmann constant, T is the absolute temperature (assumed 310 K), μ is the viscosity of water (6.95×10^{-4} kg/m · s at 310 K), and R is the molecular radius. For taxol, a value of $R = 0.5$ nm was used based on crystallographic measurements on taxotere/tubulin complexes (Nogales et al. 1998). In addition, the viscosity of water at physiological temperature (37 °C) was assumed. This yielded a diffusivity D_0 of 6.5×10^{-10} m^2/s which was then corrected for the cytoplasm (both increased cytoplasmic viscosity and macromolecular occlusion) and hindrance inside the microtubule, so that the final value of D used in the calculations was 1.8×10^{-10} m^2/s.

The diffusivity of tubulin has been measured experimentally, using fluorescence recovery after phobleaching

Table 1 Parameter estimates for diffusion and reaction in microtubules

	Taxol	$\alpha\beta$-Tubulin	Antibody (IgG)
Molecular weight (g/mol)	820	100,000	150,000
D_0 (m^2/s)[1]	6.5×10^{-10}	5.9×10^{-12}	4.3×10^{-11}
Temperature (°C)	37	25	20
K_D (nM)[2]	15	–	10
n (mM)	12	–	12
k_{on} (M^{-1} s^{-1})	2×10^9	–	1×10^5
k_{off} (s^{-1})	30	–	0.001
Cytoplasm correction, D/D_0^3	0.31	1.0 (D_0 measured in cytoplasm)	0.31
Hindrance correction, D/D_0^4	0.87	0.36	0.29

Parameters defined in text
1. Taxol diffusivity estimated by Stokes-Einstein assuming a molecular diameter of 1 nm, estimated from Nogales et al. (1998). Tubulin diffusivity measured in sea urchin egg cytoplasm by Salmon et al. (1984). Antibody (IgG) diffusivity estimated from sedimentation coefficient reported in Hasemann and Capra (1989)
2. Taxol binding constants and kinetic parameters from Caplow et al. (1994). Antibody parameters are typical of a panel of monoclonal antibodies specific for bovine serum albumin as reported by Olson et al. (1989)
3. Estimated from Kao et al. (1993). See text for discussion
4. Predicted from Nitsche and Balgi (1994) for taxol and from Bungay and Brenner (1973) for tubulin and IgG. Molecular dimensions discussed in text

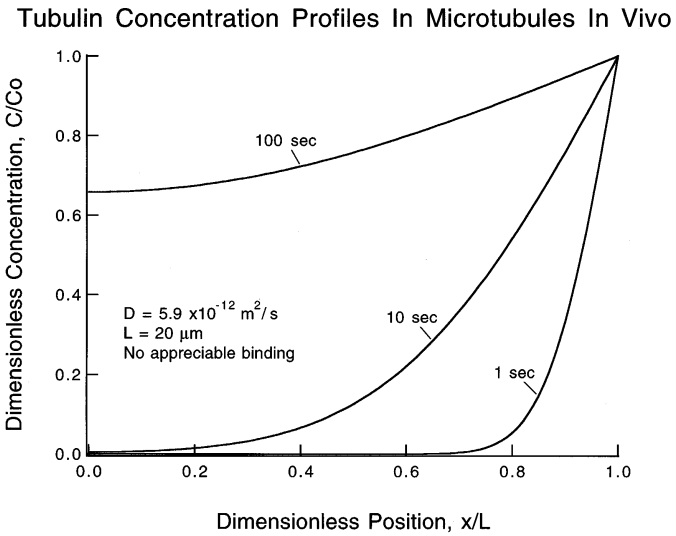

Fig. 3 Tubulin transport rates inside microtubules. Because it lacks an appreciable affinity for the microtubule wall, tubulin diffuses rapidly so that it reaches equilibrium within minutes

in sea urchin cytoplasm at 25 °C, to be 5.9×10^{-12} m^2/s (Salmon et al. 1984). This value was not corrected for the cytoplasm since the measurement was made in a living cell and correction made only for hindrance so that the final value of D used in the calculations was 2.1×10^{-12} m^2/s, about two orders of magnitude smaller than the value for taxol. Salmon et al. found an 8-fold reduction in D over that measured in water, much larger than that reported by Kao et al. for 2,7-bis-(2-carboxyethyl)-5-(and 6-)-carboxyfluorescein. This might be attributable to transient binding of tubulin the cytoplasmic structures, which would appear to retard the recovery from photobleaching (Jacobson and Wojcieszyn 1984; Kao et al. 1993). Because such transient binding of tubulin has not been experimentally demonstrated, the value estimated by Salmon et al. was used for modelling tubulin transport.

The diffusivity of IgG has been measured in water at 20 °C with a value of 4.3×10^{-11} m^2/s reported (Hasemann and Capra 1989). After correcting for the cytoplasm and hindrance effects, the final value used in the calculations was $D=3.9\times10^{-12}$ m^2/s. This gave a two-fold larger value for D than that estimated for tubulin, despite the larger size of IgG and the slightly lower temperature at which the measurements were made.

The binding parameters necessary to account for rapid, reversible binding under dilute conditions were estimated from experimental data. For taxol, Caplow et al. measured the association rate constant, k_{on}, the dissociation rate constant, k_{off}, and the dissociation equilibrium constant, K_D (=1/K), using radiolabeled taxol and guanylyl α,β-methylenediphosphonate (GMPCPP)-stabilized microtubules at nM concentrations of both taxol and tubulin (Caplow et al. 1994). These values are summarized in Table 1. Quantitative kinetic and thermodynamic data are not available for anti-acetylated tubulin antibody binding to acetylated tubulin. To estimate the parameters for antibody binding, the data of Olson et al. (1989) for a panel of anti-bovine serum albumin immunoglobulin G's (IgG's) served to approximate typical values for IgG binding to antigen. This panel had typical values of $k_{on}\sim10^5$ M^{-1} s^{-1}, $k_{off}\sim0.001$ s^{-1}, and $K_D\sim10$ nM (Olson et al. 1989).

Tubulin diffusion inside microtubules

Using the derived expression for the concentration of diffusing solute as a function of time and position (Eq. (5)) and the parameter estimates in Table 1, the concentration profile of tubulin was predicted as shown in Fig. 3. These calculations showed that tubulin concentrations inside a 20 μm long microtubule open at one end only should approach equilibrium fairly rapidly, on a time scale of minutes. These calculations are also valid for a 40 μm long microtubule open at both ends with the concentration at $x/l=0$ corresponding to the middle of the microtubule as outlined in the Model section above. An important consideration in interpreting these results is that even at equilibrium, diffusing tubulin will be very dilute a typical μM concentrations. For a 40 μm long microtubule, there will be 55 molecules of tubulin, assuming the background concentration, c_0, is 10 μM. This number of molecules is at the limit where the continuum assumption made in deriving the model begins to break down. At 10 nM tubulin there will be only a 1 in 20 chance that a single molecule will be found within the 40 μm microtubule length. To account for this fact, the ordinate in Fig. 3 can be more appropriately regarded as

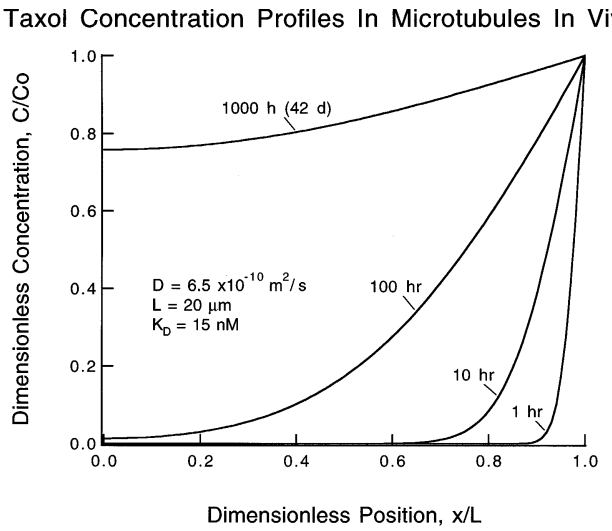

Fig. 4 Taxol transport rates inside microtubules, assuming that the taxol binding site is located on the inside of microtubules. The results assume that binding is fast, reversible, and the outside concentration, c_0, is less than K_D

the probability of finding a tubulin molecule at any position in the microtubule, relative to the probability of finding a tubulin at an arbitrary position outside the microtubule. Whether viewed deterministically in the continuum limit or probabilistically in the discrete limit, equilibrium is reached within minutes.

Taxol-diffusion with fast, reversible binding under dilute conditions

While much smaller than tubulin, taxol transport inside microtubules occurs at rates much slower than tubulin, assuming that the taxol-binding site is located on the interior surface of the microtubule. As shown in Fig. 4, it takes several days for an appreciable accumulation of taxol to develop at the base of a 20 μm microtubule with one end open or in the middle of a 40 μm microtubule with both ends open. The approach to equilibrium is retarded by the binding to the interior surface of the microtubule which occurs with a high affinity (K_D=15 nM) and a high local capacity (n=12 mM). The model predicts that it will takes months for the microtubule to be completely filled. According to Eq. (12), the diffusivity is reduced by a factor of $\sim 1/K^*$ (for $K^* \gg 1$), which for the parameters measured by Caplow et al. (1994) gives a dimensionless affinity constant of $K^*=n/K_D=(12\ \text{mM})/(15\ \text{nM})=8\times10^5$. This in turn gives a $D_{\text{eff}}=(1.8\times10^{10}\ \text{m}^2/\text{s})/(8\times10^5)=2.3\times10^{-16}\ \text{m}^2/\text{s}$ for taxol inside microtubules.

It is important to note that the model assumes dilute conditions ([taxol]$<K_D$) so that an analytical solution can be readily obtained by approximating the Langmuir isotherm as a linear isotherm. The more general Langmuir isotherm (which is nonlinear) requires numerical integration of coupled balances on both the bound and free taxol. In the case where [taxol]$>K_D$, the rates of transport will be faster than the dilute (and hence linear) case because taxol binding sites near the microtubule end will be saturated so that there will be no net binding retarding taxol transport. In addition, the model assumes the binding is fast so that molecules rapidly reach a local binding equilibrium. The average time that taxol will remain in the unbound state before rebinding is ~40 ns, corresponding to a root-mean-squared displacement of ~4 nm. Therefore, the assumption of rapid binding appears to be reasonable.

Antibody diffusion with fast, reversible binding under dilute conditions

Antibodies could potentially recognize epitopes on the interior surface of microtubules and so their transport into the microtubule lumen is required for them to bind. The physical situation is identical to that of taxol transport in that both binding and diffusion occur so that an effective diffusivity must be defined according to Eq. (9). Using the capacity (12 mM) and affinity (K_D assumed 10 nM) given for IgG in Table 1, $D_{\text{eff}}=(3.9\times10^{12}\ \text{m}^2/\text{s})/(1.2\times10^6)=3.3\times10^{-18}\ \text{m}^2/\text{s}$. Therefore the transport of antibody specific for an interior epitope is extremely slow, requiring about a year to accumulate molecules at the base of a 20 μm microtubule open at one end or in the middle of a 40 μm microtubule open at both ends as shown in Fig. 5. Given the uncertainty in the estimate of anti-acetylated antibody affinity, it is worth considering the effect of changing the affinity in the calculations. If the binding of the antibody is an order of magnitude weaker (K_D=100 nM), then it would take 100 days for the center concentration of 40 μm microtubule open at both ends to reach 75% of the equilibrium concentration. If the binding is yet another order of magnitude weaker (K_D=1 μM), the time required would be 10 days.

As with taxol, these results are based on the assumption that a linear isotherm holds, valid for [antibody]$<K_D$, and that the binding kinetics are fast compared to diffusion.

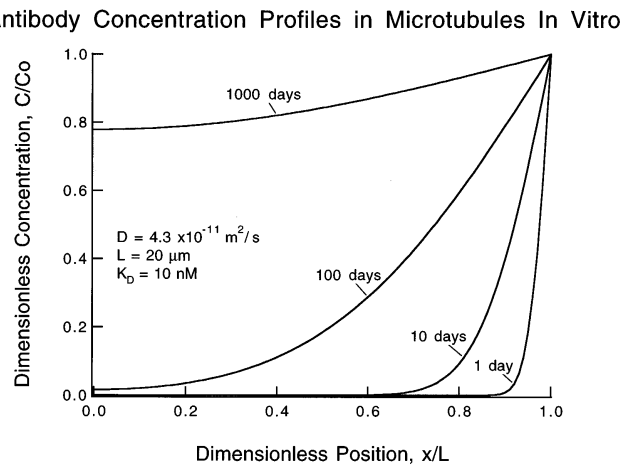

Fig. 5 Antibody transport rates inside microtubules, assuming the antibody is specific for an epitope in the interior of microtubules. The assumptions made for taxol transport apply to antibody transport also

The average time that the model antibody will remain in the unbound state before rebinding is ~1 ms, corresponding to a root-mean-squared displacement of ~2 nm. Again, the assumption of rapid binding appears to be reasonable.

Discussion

The mathematical analysis of diffusion and reaction inside microtubules shows that the rate of transport depends strongly on whether or not the diffusing molecule is capable of binding to the interior surface. If the diffusing molecule binds, as is the case for an antibody specific for an epitope on the interior of the microbubule, then the transport will be a factor of $\sim 10^6$ slower than if it does not bind (assuming an affinity of $K_D \sim 10$ nM). A second-order effect on the rate is the hindrance due to diffusion in the relatively small microtubule, whose inner diameter is roughly on the same scale as the diameter of macromolecules. Hindrance makes transport of macromolecules a factor of ~3 slower than occurs outside microtubules and is almost negligible for small molecules such as taxol (only ~20% slower).

Implications for microtubule structure

Based on an analysis of the electron crystallographic structure of $\alpha\beta$-tubulin zinc sheets, it was predicted that β-tubulin's taxol-binding site and α-tubulin's acetylation site on Lys40 are both on the inside of microtubules (Nogales et al. 1998). The present mathematical analysis seems to cast doubt on this possibility because of the long transport times required (Figs. 4 and 5) for appreciable accumulation of diffusing molecules such as taxol or an anti-acetylated tubulin antibody (antibodies specific for posttranslationally-modified tubulin are reviewed in Andreu and de Pereda (1993)). In the case of taxol, the kinetics and thermodynamics of [^{3}H]taxol binding to GMPCPP-stabilized microtubules have been characterized (Caplow et al. 1994). In this study, 5 nM [^{3}H]taxol was incubated with 7.3 nM tubulin in the form of GMPCPP microtubules. These microtubules had an average length of 7.7 μm (M. Caplow, personal communication) and were incubated with [^{3}H] taxol for 7 minutes. If the binding site were on the interior of the microtubule, then the present model predicts that binding under these conditions would be far from equilibrium with the interior 5 μm of the 7.7 μm microtubules having essentially no taxol bound after 7 minutes. Therefore, if the binding site is indeed on the interior of the microtubule, then the affinity of taxol for tubulin is greater than previously thought since not enough time was allowed for the system to reach equilbrium. Alternatively, if the binding site is on the exterior of the microtubule, then the taxol-tubulin system was presumably at equilibrium. To resolve this issue additional experiments, for example by repeating the binding experiments using longer incubation times or by directly observing the dynamics of fluorescent taxol binding to microtubules using videomicroscopy, will be required. These new experimental results can then be directly compared to the present model predictions from Eq. (5).

Recently, Evangelio et al. (1998) modelled the diffusion rate of taxol inside microtubules at high taxol concentration and found that the predicted diffusion times were much longer than those measured experimentally, consistent with the present conclusion.

Previous work with taxol binding to mitotic spindles seems to support the exterior binding site model (Salmon and Wolniak, 1984). In this study isolated spindles were preincubated for 15 minutes with 1 μM taxol (half-spindle length ~7 μm) and then taxol washed out and 100 μM Ca^{2+} simultaneously washed in. It was found that the birefringence, characteristic of the level of the microtubule polymer mass in the spindle, decreased exponentially with a half-time of ~20 minutes. That the birefringence decreased exponentially suggests that the microtubules had reached equilibrium with the taxol by the end of the 15 minute preincubation period. Based on the present model results, if the taxol binding site is on the interior of the microtubules, then it would be expected that the birefringence would slowly decrease until the more labile interior regions of the spindle microtubules were exposed at which point the birefringence would rapidly decrease. It should be noted that the experiments were conducted using 1 μM taxol, while the present model results are only strictly valid at nM concentrations (assuming $K_D = 15$ nM).

Another possible mechanism for taxol transport and binding is that taxol might be able to squeeze its way through gaps between tubulin subunits in the microtubule lattice. In this model the gaps would need to be ~1 nm or larger in diameter, a plausible distance based on current structural models for the microtubule lattice (Nogales et al. 1998). This possibility could be tested experimentally, possibly by covalently linking taxol to a particle too large to pass through the microtubule lattice gaps. Such a taxol-particle should not be able to bind to the microtubule if the binding site is located on the interior of the microtubule, but should be able to bind if the binding site is located on the exterior surface.

In the case of antibody binding, the very long times required for appreciable accumulation of antibodies inside a microtubule also appears to cast doubt on the prediction that recognized epitopes such as the acetylated-Lys40 of α-tubulin are located on the interior of microtubules. In labelling experiments, ~30 nM concentrations of anti-acetylated tubulin antibodies were used in a 30 minute incubation at room temperature to label microtubules in permeabilized and fixed cells (Schulze et al. 1987). Fluorescence microscopy revealed extensive labelling of microtubules, some with labelling lengths approaching 10 μm. Based on the present mathematical analysis, these results are inconsistent with a model where the acetylation site is on the interior of microtubules. In addition, it would be expected that the antibodies themselves would contribute to additional hindrance, owing to their relative large size and would retard passage of molecules into the microtubules once they had bound near the microtubule tip. It seems very

unlikely that an antibody could squeeze through gaps in the microtubule lattice. One alternative mechanism for transport into the microtubule lumen is that the fixation associated with the immunostaining preparation damages the microtubule lattice so that gaps are created that allow passage of antibodies. As few as one or two tubulin dimers lost from the lattice could provide a gap large enough for an antibody to pass through the wall. Experimentally this could be tested by exposing unfixed microtubules directly to anti-acetylated tubulin antibodies and determine whether binding occurs.

Implications for controlled-release drug delivery

The slow transport rates in microtubules suggest that microtubules might serve as vehicles for drug delivery in controlled-release applications, particularly if the therapeutic drug binds to the interior of the microtubule. These drug molecules could be loaded into microtubules at high (mM) concentrations during microtubule assembly and the microtubules stabilized by GMPCPP. Implanted or injected microtubules would then slowly release the drug over time scales of days to months, depending on the size of the molecule, the affinity of the drug for tubulin, and the length of the microtubules. To achieve kinetics closer to the desired zero-order release kinetics, the microtubules could be preincubated before transfer to the patient to reduce the concentration near the microtubule tips. The controlled-release strategy might be especially beneficial to deliver taxol which has poor solubility in aqueous media and therefore its administration is difficult. In the particular case of taxol it would be especially appropriate if the taxol binding site is located on the interior of the microtubule. Finally, the model results generally apply to diffusion of molecules, including therapeutic drugs, through narrow one-dimensional channels in cells such as membrane transport channels and gap junctions.

Acknowledgements The author wishes to thank Ken Downing for stimulating this work. The author is also grateful to Michael Caplow for sharing unpublished data and to Ted Salmon for helpful comments. The work was supported by a Biomedical Engineering Research Grant from the Whitaker Foundation.

References

Amos LA (1979) Structure of microtubules. In: Roberts K, Hyams JS (eds) Microtubules. Academic Press, London

Andreu JM, de Pereda JM (1993) Site-directed antibodies to tubulin. Cell Motil Cytoskel 26: 1–6

Berg H (1993) Random walks in biology. Princeton University Press, Princeton, NJ

Bungay PM, Brenner H (1973) The motion of a closely-fitting sphere in a fluid-filled tube. Int J Multiphase Flow 1: 25–56

Caplow M, Shanks J, Ruhlen R (1994) How taxol modulates microtubule assembly. J Biol Chem 269: 23399–23402

Crank J (1975) The mathematics of diffusion, 2nd edn. Oxford University Press, Oxford

Deen WM (1987) Hindered transport of large molecules in liquid-filled pores. AIChE J 33: 1409–1425

Dogterom M, Maggs AC, Leibler S (1995) Diffusion and formation of microtubule asters: physical processes versus biochemical regulation. Proc Natl Acad Sci USA 92: 6683–6688

Evangelio JA, Abal M, Barasoain I, Sonto AA, Lillo MP, Acuna AN, Amatauerri F, Andreu JM (1998) Fluorescent taxoids as probes of the microtubule cytoskeleton. Cell Motil Cytoskel 39: 73–90

Hasemann CA, Capra JD (1989) Immunoglobulins: structure and function. In: Paul WE (ed) Fundamental immunology. Raven Press, New York

Jacobson K, Wojcieszyn J (1984) The translational mobility of substances within the cytoplasmic matrix. Proc Natl Acad Sci USA 81: 6747–6751

Kao HP, Abney JR, Verkman AS (1993) Determinants of the translational mobility of a small solute in cell cytoplasm. J Cell Biol 120: 175–184

Nitsche JM, Balgi G, (1994) Hindered diffusion of spherical solutes within circular cylindrical pores. Ind Eng Chem Res 33: 2242–2247

Nogales E, Wolf SG, Downing KH (1998) Structure of the $\alpha\beta$ tubulin dimer by electron crystallography. Nature 391: 199–203

Odde DJ (1997) Estimation of the diffusion-limited rate of microtubule assembly. Biophys J 73: 88–96

Olson WC, Spitznagel TM, Yarmush ML (1989) Dissociation kinetics of antigen-antibody interactions: studies on a panel of anti-albumin monoclonal antibodies. Mol Immunol 26: 129–136

Renkin EM (1954) Filtration, diffusion, and molecular sieving through porous cellulose membranes. J General Physiol 38: 225

Salmon ED, Saxton WM, Leslie RJ, Karow ML, McIntosh JR (1984) Diffusion coefficient of fluorescein-labeled tubulin in the cytoplasm of embryonic cells of a sea urchin: video image analysis of fluorescence redistribution after photobleaching. J Cell Biol 99: 2157–2164

Salmon ED, Wolniak SM (1984) Taxol stabilization of mitotic spindle microtubules. Cell Motil 4: 155–167

Schulze E, Asai DJ, Bulinski JC, Kirschner M (1987) Posttranslational modification and microtubule stability. J Cell Biol 105: 2167–2177